ORGANIC LETTERS

2009
Vol. 11, No. 15
3378−3381

Cu^{2+} Ion-Induced Self-Assembly of Pyrenylquinoline with a Pyrenyl Excimer Formation

Hyo Sung Jung,[†] Mirae Park,[‡] Do Young Han,[†] Eunmi Kim,[‡] Chewook Lee,[‡] Sihyun Ham,[*,‡] and Jong Seung Kim[*,†]

Department of Chemistry, Korea University, Seoul 136-701, Korea, and Department of Chemistry, Sookmyung Women's University, Seoul 140-742, Korea

sihyun@sookmyung.ac.kr; jongskim@korea.ac.kr

Received June 1, 2009

ABSTRACT

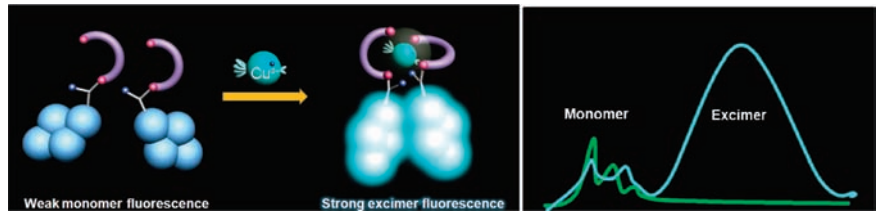

Synthesis of a novel pyrene derivative sensor (1) and its intermolecular binding pattern to Cu^{2+} in CH_3CN were investigated. Upon Cu^{2+} binding, the sensor exhibited a strong *static* excimer emission at 460 nm, along with a weak monomer emission at 388 nm. The excimer emission intensity induced by the Cu^{2+} ion declined as the spacer length between the pyrene and quinolinylamide unit increased. The Cu^{2+} ion-induced self-assembled pyrenyl excimer formation is rationalized by fluorescence experiments and theoretical DFT calculations.

A chemosensor is a compound that renders a significant change in electrical, electronic, magnetic, or optical signals when it binds to a specific guest counterpart. Of those sensors, fluorescent chemosensors have several advantages over other methods given their sensitivity, specificity, and real-time monitoring with fast response time.[1] Recently, the development of fluorescent chemosensors capable of selective recognition and sensing of metal ions is one of the most challenging fields from the vantage of organic and supramolecular chemistry.[2] In particular, under certain circumstances, it is highly necessary to selectively sense heavy metal ions such as mercury, lead, and copper ions.[3] Copper(II) plays an important role in various fields.[4] However, exposure to a high level of copper, even for a short period of time, can cause gastrointestinal disturbance, while long-term exposure can cause liver or kidney damage.[5] For these reasons, the past few years have witnessed a number of reports on the design and synthesis of fluorescent sensors for the detection of Cu^{2+} ions. For most of the reported Cu^{2+} fluorescent sensors, the binding of the Cu^{2+} ion causes a fluorescence quenching due to its paramagnetic nature,[6] although a few

[†] Korea University.
[‡] Sookmyung Women's University.

(1) (a) Lai, C.-Y.; Trewyn, B. G.; Jeftinija, D. M.; Jeftinija, K.; Xu, S.; Jeftinija, S.; Lin, V. S.-Y. *J. Am. Chem. Soc.* **2003**, *125*, 4451. (b) Numata, M.; Li, C.; Bae, A.-H.; Kaneko, K.; Sakurai, K.; Shinkai, S. *Chem. Commun.* **2005**, 4655.

(2) (a) de Silva, A. P.; Gunaratne, H. Q. N.; Gunnlaugsson, T.; Huxley, A. J. M.; McCoy, C. P.; Rademacher, J. T.; Rice, T. E. *Chem. Rev.* **1997**, *97*, 1515. (b) Valeur, B.; Leray, I. *Coord. Chem. Rev.* **2000**, *205*, 3. (c) Prodi, L.; Bolletta, F.; Montalti, M.; Zaccheroni, N. *Coord. Chem. Rev.* **2000**, *205*, 59. (d) Fabbrizzi, L.; Poggi, A. *Chem. Soc. Rev.* **1995**, *24*, 197. (e) Kim, J. S.; Quang, D. T. *Chem. Rev.* **2007**, *107*, 3780. (f) Kim, H. N.; Lee, M. H.; Kim, H. J.; Kim., J. S.; Yoon, J. *Chem. Soc. Rev.* **2008**, *37*, 1465.

(3) (a) Okamoto, A.; Ichiba, T.; Saito, I. *J. Am. Chem. Soc.* **2004**, *126*, 8364. (b) Lee, J. W.; Jung, H. S.; Kwon, P. S.; Kim, J. W.; Bartsch, R. A.; Kim, Y.; Kim, S.-J.; Kim, J. S. *Org. Lett.* **2008**, *10*, 3801.

(4) (a) Rurack, K.; Kollmannsberger, M.; Resch-Genger, U.; Daub, J. *J. Am. Chem. Soc.* **2000**, *122*, 968. (b) Moon, S. Y.; Cha, N. R.; Kim, Y. H.; Chang, S.-K. *J. Org. Chem.* **2004**, *69*, 181.

(5) (a) Barceloux, D. G.; Barceloux, D. *J. Toxicol.-Clin. Toxicol.* **1999**, *37*, 217. (b) Zhang, X. B.; Peng, J.; He, C.-L.; Shen, G.-L.; Yu, R.-Q. *Anal. Chim. Acta* **2006**, *567*, 189. (c) Sarkar, B. In *Metal ions in biological systems*; Siegel, H., Siegel, A., Eds.; Marcel Dekker: New York, 1981; Vol.12, pp 233. (d) Que, E. L.; Domaille, D. W.; Chang, C. J. *Chem. Rev.* **2008**, *108*, 1517.

10.1021/ol901221q CCC: $40.75
Published on Web 07/10/2009

sensors where the binding of the Cu^{2+} ion causes an increase in the fluorescence have also been reported.[7]

As a fluorescent probe, pyrene has often been effectively used because its emission property is sensitive to its local environment.[8] Depending on the relative proximity between pyrene moieties, unique monomer and excimer emissions are observed at considerably different wavelengths, through which structural information can be analyzed. Taking advantage of such unique physical properties of the pyrene, we have designed a series of pyrenylamide derivatives able to form self-assembled dimeric structures upon a certain metal cation to give a Py−Py* excimer fluorescence band rarely studied. From this, new guidelines to develop chemosensor materials can be formulated.

Here, we report the synthesis of new pyrene-derived Cu(II)-selective fluorescent sensor **1** and its binding mechanism toward Cu(II) by fluorescence spectroscopy and theoretical DFT calculations.

The synthetic pathways of fluorogenic molecules **1**−**4** are summarized in Scheme S1 (Supporting Information). Compounds **1**−**3** were synthesized in 63, 64, and 65% yields, respectively. As depicted in Figure 1, to optimize the sensing

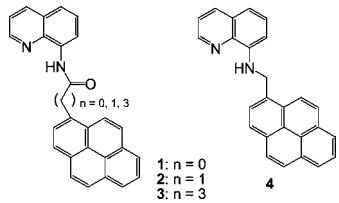

Figure 1. Pyrenylquinoline derivatives **1**−**4**.

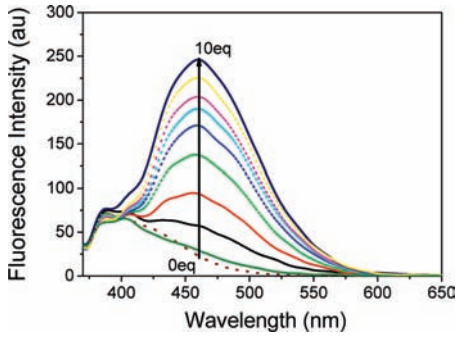

Figure 2. Fluorescence titration spectra of **1** (6.0 μM) in CH_3CN upon addition of various amounts of $Cu(ClO_4)_2$ (0, 1, 2, 3, 4, 5, 6, 7, 8, 9, and 10 equiv) at an excitation of 360 nm.

efficiency of the pyrenyl-8-aminoquinoline toward the Cu(II) ion with respect to excimer formation of the pyrene moiety upon the metal cation, the spacer length (n = 0, 1, 3) between the pyrene and quinolinylamide group was varied. To envision the binding mode of the 8-aminoquinoline nitrogen and carbonyl group to Cu(II), **4** was also synthesized in 44% yield. The structures of **1**−**4** were confirmed by ^1H NMR, ^{13}C NMR, and FAB-MS (Figures S8−S20, Supporting Information).

Figure 2 shows the gradual change of the fluorescence spectra of **1** upon addition of Cu^{2+}. Addition of Cu^{2+} produced a new emission band centered at 460 nm with increasing intensity, which is in stark contrast to other metal cations where no significant fluorescence changes were observed (Figure 3). By measuring the emission maximum

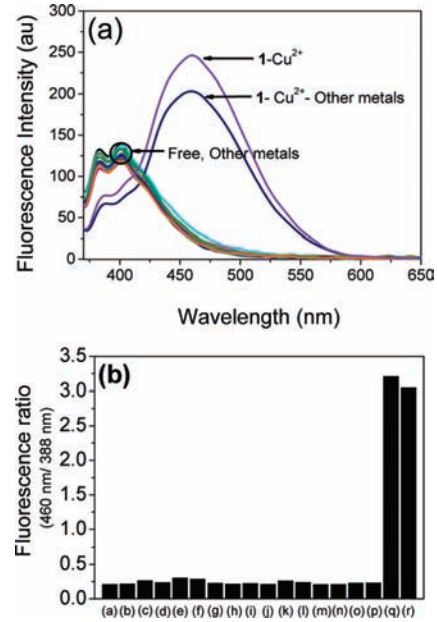

Figure 3. (a) Fluorescence emission spectra of **1** (6.0 μM) upon addition of ClO_4^- salts of Li^+, Na^+, K^+, Rb^+, Cs^+, Ag^+, Cd^{2+}, Mg^{2+}, Sr^{2+}, Ba^{2+}, Zn^{2+}, Ca^{2+}, Pb^{2+}, Co^{2+}, Hg^{2+}, Cu^{2+}, and Cu^{2+} + other metals (10 equiv, respectively) in CH_3CN with excitation at 360 nm. (b) Histogram of metal ion selectivity with **1**. ((a) none, (b) Li^+, (c) Na^+, (d) K^+, (e) Rb^+, (f) Cs^+, (g) Ag^+, (h) Cd^{2+}, (i) Mg^{2+}, (j) Sr^{2+}, (k) Ba^{2+}, (l) Zn^{2+}, (m) Ca^{2+}, (n) Pb^{2+}, (o) Co^{2+}, (p) Hg^{2+}, (q) Cu^{2+}, (r) Cu^{2+} + other metals (10 equiv, respectively)).

of **1**-Cu^{2+}, the fluorescence change of **1** responded to the range of 0−60 μM of [Cu^{2+}]. It was then found that **1** shows a 1.0 μM detection limit, satisfactory to U.S. EPA limits (~20 μM) of Cu^{2+} detection in drinking water.[9] Using the fluorescence titration data, the binding constant of **1** with Cu^{2+} in aqueous solution was found to be 5.42×10^5.[10]

(6) (a) Jung, H. S.; Kwon, P. S.; Lee, J. W.; Kim, J. I.; Hong, C. S.; Kim, J. W.; Yan, S.; Lee, J. Y.; Lee, J. H.; Joo, T.; Kim, J. S. *J. Am. Chem. Soc.* **2009**, *131*, 2008. (b) Varnes, A. W.; Dodson, R. B.; Wehry, E. L. *J. Am. Chem. Soc.* **1972**, *94*, 946. (c) Kemlo, J. A.; Shepherd, T. M. *Chem. Phys. Lett.* **1977**, *47*, 158. (d) Rurack, K.; Resch, U.; Senoner, M.; Daehne, S. *J. Fluoresc.* **1993**, *3*, 141.

(7) (a) Zhang, X.; Shiraishi, Y.; Hirai, T. *Org. Lett.* **2007**, *9*, 5039. (b) Xu, Z.; Xiao, Y.; Qian, X.; Cui, J.; Cui, D. *Org. Lett.* **2005**, *7*, 889. (c) Swamy, K. M. K.; Ko, S.-K.; Kwon, S. K.; Lee, H. N.; Mao, C.; Kim, J.-M.; Lee, K.-H.; Kim, J.; Shin, I.; Yoon, J. *Chem. Commun.* **2008**, 5915. (d) Yu, M.; Shi, M.; Chen, Z.; Li, F.; Li, X.; Gao, Y.; Xu, J.; Yang, H.; Zhou, Z.; Yi, T.; Huang, C. *Chem. Eur. J.* **2008**, *14*, 6892.

(8) (a) Nishizawa, S.; Kato, Y.; Teramae, N. *J. Am. Chem. Soc.* **1999**, *121*, 9463. (b) Sahoo, D.; Narayanaswami, V.; Kay, C. M.; Ryan, R. O. *Biochemistry* **2000**, *39*, 6594.

(9) The U.S. Environmental Protection Agency (EPA) has set the limit of copper in drinking water to be 1.3 ppm (~20 μM).

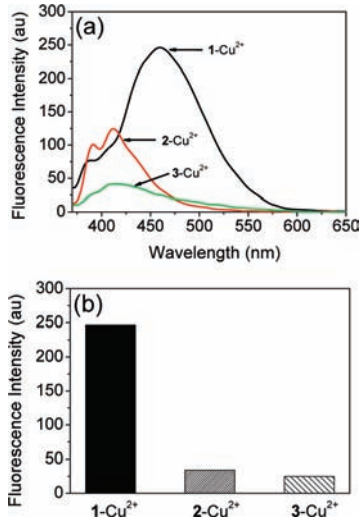

Figure 4. (a) Fluorescence spectra of **1**−**3** (6.0 μM, respectively) upon addition of $Cu(ClO_4)_2$ (10 equiv, respectively) in CH_3CN with excitation at 360 nm. (b) Relative responses at 460 nm of **1** − **3** (6.0 μM, respectively) upon addition of $Cu(ClO_4)_2$ (10 equiv, respectively) in CH_3CN with excitation at 360 nm.

Complexation abilities of **1** toward the metal cations were examined via absorption spectral changes of **1** upon addition of various metal cations (Figure S1, Supporting Information). The band broadening and red-shift (color change from colorless to orange) in the UV−vis spectra of **1** upon the addition of Cu^{2+} ions were attributable to the favorable intermolecular $\pi-\pi$ stacked dimerization of the two pyrenes in the ground state.[11]

To quantify the complexation ratio between **1** and the Cu^{2+} ion, the Job plot measurement was carried out by varying the concentration of both **1** and the Cu^{2+} ion (Figure 5). The

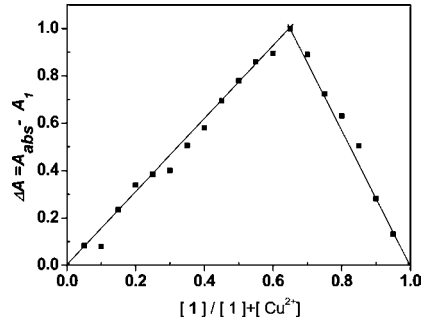

Figure 5. Job plot of a 2:1 complex of **1** and the Cu^{2+} ion, where the difference in absorbance intensity at 360 nm was plotted against the mole fraction of **1** at an invariant total concentration of 10 μM in CH_3CN.

maximum point appears at the mole fraction of 0.65, close to the typical ligand mole fraction (0.66) for a 2:1 ligand-to-metal complex. The mass spectrum also confirms formation of the 2:1 complex (Figure S12, Supporting Information) where there is a major peak at *m*/*z* 830.87, corresponding to 2(**1**) + Cu^{2+} + Na^{+}.

For Cu(II)-induced pyrene excimer formation, it is first assumed that the interaction of the quinolinylamide group with the Cu^{2+} ion induces an intermolecular Py−Py* interaction with **1**, which causes both color and fluorescence changes. Quinolymethylpyrene **4**, lacking a carbonyl group, was prepared to discern any decisive role of the carbonyl group in Cu(II) ion complexation followed by pyrenyl excimer formation. Upon addition of the Cu^{2+} ion, a solution of **4** gave rise to negligible changes in the fluorescent spectra (Figure S4, Supporting Information). From this vantage point, it should be noted that both the quinoline host and pyrenylamide portions play an important role in selective Cu(II) ion encapsulation by a 2:1 complexation mode, leading to the observed pyrene excimer band at 460 nm.

To verify a crucial influence of the spacer length of the probe on the Py−Py* interaction upon the addition of the Cu^{2+} ion, **1**−**3** were synthesized with variations in length (n = 0, 1, 3) between the pyrene and quinolinylamide groups and fluorescence changes with the Cu^{2+} ion tested. As seen in Figure 4, unlike **1**, neither shows any distinct excimer emission upon addition of the Cu^{2+} ion. These results precisely indicate that no methylene spacer between the pyrene and carbonyl unit optimizes the intermolecular Py−Py* formation to show an intense static excimer band. In the presence of 10 equiv of Cu^{2+}, the excimer emission intensity of **1** became ∼8 times greater than that of probe **2** or **3**.

To elucidate the molecular origin of the distinct fluorescence behaviors of **1**−**3** upon addition of the Cu^{2+} ion, density functional theory calculations were executed for the energy minimized structures of **1**−**3** at the B3LYP/3-21G* level of theory.[12] The global minima structures for the monomers of **1**−**3** are shown in Figure S6 (Supporting Information). Due to the 2:1 ligand-to-metal complexation behavior determined by both the mass spectrum and the Job plot, the dimers of **1**−**3** with and without the Cu^{2+} ion were executed to the energy minimization. The lowest energy structures for dimers of **1**−**3** are represented in Figure 6.

Without the spacer between the pyrene and quinolinylamide groups, as in the case of **1**, the H-bond is fairly weak with a distance of 2.5 Å due to the steric hindrance between the proximate pyrene groups, as shown in Figure 6(a). However, in the case of **2** and **3**, with n = 1 and 3, stable H-bonding between two amide groups is available to form stable dimers at a distance of 2.1 Å in the dimers of **2** and

(10) (a) Benesi, H. A.; Hildebrand, J. H. *J. Am. Chem. Soc.* **1949**, *71*, 2703. (b) Barra, M.; Bohne, C.; Scaiano, J. C. *J. Am. Chem. Soc.* **1990**, *112*, 8075.

(11) Kim, H. J.; Kim, S. K.; Lee, J. Y.; Kim, J. S. *J. Org. Chem.* **2006**, *71*, 6611.

(12) An initial conformational analysis for each molecular system was first performed by molecular dynamics (MD) simulation using SANDER module of AMBER program employing parm99 force field.[13] From the MD simluation trajectory, a total of 200 structures were collected which were then subjected to the following optimization procedure using the AM1 semiempirical method[14] to find the energy minima that would be used as initial structures for the density functional theory (DFT) calculations. The DFT calculations were performed at the B3LYP/3-21G* level[15] using the Gaussian 03 package.[16] Frequency calculations were performed to verify the identity of each stationary point as a minimum. For the thermodynamic stability comparison, single point energy calculation was executed at the MPWB1K/3-21G* level using B3LYP/3-21G* optimized geometry.

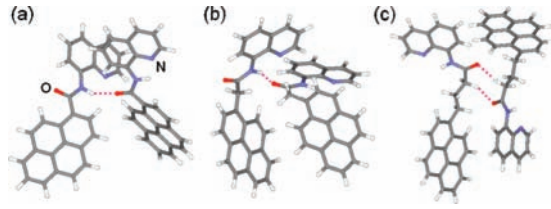

Figure 6. Global minima structures for the dimers of (a) **1**, (b) **2**, and (c) **3**, optimized at the B3LYP/3-21G* level. Hydrogen bonds are depicted as a pink dotted line.

2.1 and 2.0 Å in the dimers of **3**. Consequently, the binding energy for the dimer of **3** with two H-bonds was highest at 22.4 kcal/mol, compared to those of **2** and **1** at 19.4 and 12.0 kcal/mol at the MPWB1K/3-21G*//B3LYP/3-21G* level, respectively. On the basis of this calculation, addition of the Cu^{2+} ion to the dimers of **2** and **3** will disrupt the stable H-bonding between the two amide units. Subsequently, it is expected that addition of Cu^{2+} ions to the dimers of **2** and **3**, which would perturb the stable electrostatic interactions between two monomer units, may be thermodynamically less favorable compared to addition to the dimer of **1**.

The lowest-energy conformations for the Cu^{2+} complexes of **1**−**3** were located and represented in Figure 7(a) and S6

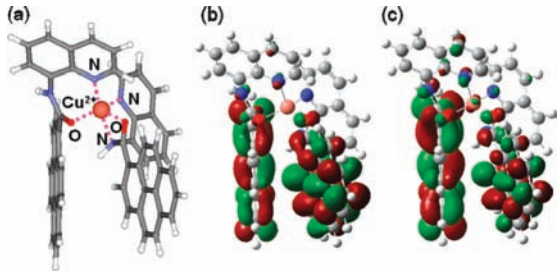

Figure 7. (a) Lowest energy structure for the **1**−Cu^{2+} complex, (b) HOMO of the **1**−Cu^{2+} complex, and (c) LUMO of the **1**−Cu^{2+} complex.

(Supporting Information). As shown in Figure 7(a), the Cu^{2+} ion is coordinated to two oxygens and three nitrogens with an average distance of 1.99 Å. The common structural feature depicted in all three Cu^{2+} complexes of **1**−**3** is that the Cu^{2+} ion is most effectively recognized by the amide oxygen next to the pyrene group. Atomic charge calculations using natural population analysis (NPA)[17] were performed. The electron density change was most distinctively detected in the amide oxygen upon Cu^{2+} ion complexation to **1**−**3**.

To further understand the fluorescence changes upon addition of the Cu^{2+} ion, a time-dependent density functional theory (TDDFT) calculation was executed for Cu^{2+} complexation to **1**−**3**. The molecular orbital energies and associated electronic transitions were calculated from the optimized geometry of the S_0 state at the TDDFT/B3LYP/3-21G* level. Several studies have shown that hybrid functionals give the best results for evaluating electronic transitions in organic molecules.[18] On the basis of the TDDFT/B3LYP/3-21G* calculations, the efficient HOMO to LUMO excitations from one pyrene to the other facing pyrene (Py−Py* interaction) presumably contribute to the strong fluorescence excimer bands for the **1**−Cu^{2+} complex. Conversely, no pyrene excimer transition was observed in the Cu^{2+} ion complexes of **2** and **3**, as shown in Figure S7 (Supporting Information). To this end, the theoretical DFT calculation results are in excellent agreement with the observed experimental observation that the distinct fluorescence excimer emission upon addition of the Cu^{2+} ion is associated with the Py−Py* interaction in the **1**−Cu^{2+} complex, whereas no such interaction is displayed in the Cu^{2+} complex of **2** and **3**.

In summary, we presented a new pyrene-based Cu^{2+} indicator (**1**) that functions both as a naked-eyed and fluorogenic probe for metal cations. Compound **1** coordinates Cu^{2+} with 2:1 complex stoichiometries, as deduced from the Job's plot analysis, mass spectra, and fluorescence behavior. Addition of Cu^{2+} to **1** gave a significant excimer emission through a 2:1 ligand-to-metal complex. On the basis of the synthesis and DFT calculations of various pyrenylquinolines presented in this report, the predominant factor in the rational design of a fluorescence probe of modulated pyrenylquilnolines for Cu^{2+} ion sensing is to maintain the intramolecular distance between the pyrene and quinoline amide groups at a minimum. This allows for eminent Py−Py* interactions, as in **1**.

Acknowledgment. This work was supported by a SRC (KOSEF) grant (No. R11-2005-008-00000-0) and the CRI Program of the MEST. This research was also suppoprted by the grant (R01-2006-10696) from KOSEF, in which main calculations were performed by using the supercomputing resource of the Korea Institute of Science and Technology Information (KSC-2007-S00-0018).

Supporting Information Available: Synthetic details, additional NMR, UV, and emission spectral data, and DFT optimized structures for the monomers of **1**∼**3** and **2**−Cu^{2+} and **3**−Cu^{2+} complexes. This material is available free of charge via the Internet at http://pubs.acs.org.

OL901221Q

(13) Case, D. A.; Darden, T.; Pearlman, D. A.; Caldwell, J. W.; Cheatham, T. E., III; Simmerling, C. L.; Wang, J.; Duke, R. E.; Luo, R.; Merz, K. M.; Crowley, M.; Walker, R. C.; Zhang, W.; Wang, B.; Hayik, S.; Roitberg, A.; Seabra, G.; Wong, K. F.; Paesani, F.; Wu, X.; Brozell, S.; Tsui, V.; Gohlke, H.; Yang, L.; Tan, C.; Mongan, J., Hornak, V.; Cui, G.; Beroza, P.; Mathews, D. H.; Schafmeister, C.; Ross, W. S.; Kollman, P. A. *AMBER 9*; University of California: San Francisco, 2006.

(14) (a) Dewar, M. J. S.; Thiel, W. *J. Am. Chem. Soc.* **1977**, *99*, 4899. (b) Dewar, M. J. S.; Zoebisch, E. V.; Healy, E. F.; Stewart, J. J. P. *J. Am. Chem. Soc.* **1985**, *107*, 3902.

(15) Becke, A. D. *J. Chem. Phys.* **1993**, *98*, 5648.

(16) Frisch, M. J., et al. *Gaussian 03*; Gaussian, Inc.: Wallingford CT, 2004. See Supporting Information for full reference.

(17) Rao, J. S.; Dinadayalane, T. C.; Leszczynski, J.; Sastry, G. N. *J. Phys. Chem. A* **2008**, *112*, 12944.

(18) (a) Tokura, S.; Yagi, K.; Tsuneda, T.; Hirao, K. *Chem. Phys. Lett.* **2007**, *436*, 30. (b) Wilberg, K. B.; Stratmann, R. E.; Frisch, M. J. *Chem. Phys. Lett.* **1998**, *297*, 60. (c) Adamo, C.; Barone, V. *Chem. Phys. Lett.* **2000**, *330*, 152. (d) Choi, J. K.; Lee, A.; Kim, S.; Ham, S.; No, K.; Kim, J. S. *Org. Lett.* **2006**, *8*, 1601. (e) Kim, H. J.; Quang, D. T.; Hong, J.; Kang, G.; Ham, S.; Kim, J. S. *Tetrahedron* **2007**, *63*, 10788. (f) Kim, H. J.; Hong, J.; Hong, A.; Ham, S.; Lee, J. H.; Kim, J. S. *Org. Lett.* **2008**, *10*, 1963.